Songklanakarin J. Sci. Technol.
40 (2), 354-358, Mar. - Apr. 2018

http://www.sjst.psu.ac.th

Original Article

Structural properties of mechanically ball-milled porous silicon

Chanika Puridetvorakul[1, 2], Wandee Onreabroy[2, 3], and Tula Jutarosaga[2, 3*]

[1] *Division of Materials Technology, School of Energy, Environment and Materials, King Mongkut's University of Technology Thonburi, Thung Khru, Bangkok, 10140 Thailand*

[2] *Department of Physics, Faculty of Science, King Mongkut's University of Technology Thonburi, Thung Khru, Bangkok, 10140 Thailand*

[3] *Thin Film Technology Research Laboratory, Thailand Center of Excellence in Physics, The Office of the Higher Education Commission, Ratchathewi, Bangkok, 10400 Thailand*

Received: 27 June 2016; Revised: 5 December 2016; Accepted: 4 January 2017

Abstract

A simple powder technique with hydrofluoric (HF) acid leaching technique was presented for the fabrication of bulk porous silicon (PS). Silicon wafers were crushed, ball milled for various milling times and pressed into pellets under the pressure of 4,000 psi (276 bar). Samples were annealed in H_2/Ar and in air. Structural properties of PS were investigated using X-ray diffraction technique, scanning electron microscopy, and Fourier-transform infrared spectroscopy. Crystalline size of Si nanoparticles decreased with increase of milling time and can be improved after mechanical pressing and annealing. Obtained PS pellets had uniform porosity. Porosity of the specimen could be significantly increased with the combination of annealing in air to promote the oxide layer on the silicon nanoparticles and HF leaching to form voids by removing the created oxide layer. Preliminary results showed that the percent porosity can be increased up to 43.6%.

Keywords: ball milling, hydrofluoric leaching, nanostructure materials, porous silicon

1. Introduction

Silicon (Si) materials have attracted much interest due to their applications in various fields such as Si-nanowire solar cells (Moiz *et al.*, 2012; Stelzner *et al.*, 2008), amorphous thin films solar cells (Ji *et al.*, 2011), photodetectors (Kurdi *et al.*, 2003) and materials for optical communication (Ebrahimy *et al.*, 2015). Porous Silicon (PS) materials, one among many nanostructure materials, have been applied for various applications, for examples in the anti-reflection coating layers in photovoltaic application (Salman *et al.*, 2012). It was also found that the energy gap of PS samples showed an enlargement compared to that of bulk crystalline Si (Naddaf & Hamadeh, 2009). The difference of the energy gap caused the photovoltaic effect in the hetero-junction PS/p-silicon (Smestad *et al.*, 1992).

The fabrication process of PS material has been developed continuously due to its varieties of applications. To date, a popular method of preparing PS structures is electrochemically etching (Naddaf & Hamadeh, 2009; Salman *et al.*, 2011; Smestad *et al.*, 1992). However, powder metallurgy method with high-energy ball milling followed by pressing and annealing gives the advantage of uniform porosity which can be obtained regardless the direction of the bulk samples (Serov, 2014). While, the electrochemical etching provides the columnar structures perpendicular to the surface of Si wafers (Kim & Cho, 2012). Ball milling method have been observed to fabricate silicon nanoparticles (Jakubowicz *et al.*, 2007; Russo *et al.*, 2011), but not compacted porous Si pellets.

Besides the ball-milling method, to fabricate high specific surface area Si nanoparticles there was a report on the mechanochemical reduction process of silicon monoxide

*Corresponding author
Email address: tula.jut@mail.kmutt.ac.th

(SiO) and magnesium silicide (Mg_2Si). The oxide can be reduced and after HF leaching high specific surface area Si nanoparticles can be produced (Epur *et al.*, 2013). However, fabrication process of PS with the combination of powder metallurgy method and acid leaching has rarely been studied.

In this work, without other materials like the earlier report (Epur *et al.*, 2013), a simple process consisting of mechanical ball milling of silicon wafer, pressing into pellet, annealing in different ambient and following by the diluted HF etching was presented to form a high surface area PS pellets. More specifically, as shown in Figure 1, our concept was to remove the silicon dioxide created by the annealing process at the surface of silicon particles in PS pellets, Figure 1(a), to form larger voids between Si nanoparticles, Figure 1(b), to increase the porosity. In this work, a simple HF etching was purposed to increase these void and porosity.

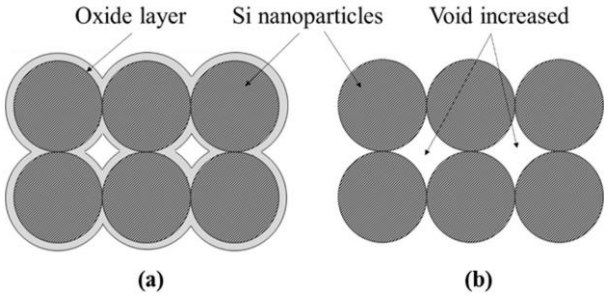

Figure 1. Schematic diagram of (a) annealed porous silicon (PS) and (b) the HF-leached PS.

2. Materials and Methods

2.1 Sample preparation

A simple powder technique for the preparation of porous silicon (PS) was used in this experiment. The (100) p-type silicon wafers with resistivity 0.001-0.005 Ωcm were crushed for five minutes, mechanically ball-milled for 1, 3, 8, 12, 18, and 21 hours and pressed into pellets with a small addition of 5% polyvinyl alcohol (PVA) binder solution under the pressure of 4,000 psi (276 bar). Pellets had a diameter of about 10 mm with the thickness of about 2 mm. The pellets were then annealed at 700 °C in H_2/Ar (5% H_2 in 95% Ar ambient) for 30 minutes in order to prevent oxide formation. Also, specimens with the milling time of one hour were pre-pared and annealed at a fixed selected temperature of 900 °C for 0.5, 1, 2, and 3 hours in air to oxidize the surface. The oxide was then removed with 5% HF solutions for 30 minutes to increase the porosity. The fabrication parameters are shown in Table 1.

Table 1 Fabrication parameters.

Milling time (hours)	Annealing time (hours)	Annealing Condition
1, 3, 8, 12, 18, 21	0.5	700 °C in H_2/Ar (95% Ar)
1	0.5, 1.0, 3.0	900 °C in air

2.2 Characterization

The crystal structures and morphological properties of the specimens were characterized using the X-ray diffraction (XRD) technique and the scanning electron microscopy (SEM) technique. D8 Discover, Bruker AXS with the Cu K_α radiation was used to analyze the structures of the pellets. Patterns were obtained in the 2θ ranging from 20° to 80° with the step size of 0.2 °/s at room temperature. Average crystalline sizes of various specimens were estimated from the Scherer's formula using the strongest diffraction peaks of (111) plane. The lattice constant (a) was calculated using the published Miller indices (h k l) of the reflection according to the position observed in the XRD spectra. The formation of silicon oxide was investigated by Fourier-transform infrared spectroscopy (FTIR).

In order to calculate the total porosity including both open and closed pores, the mass and the dimension of the prepared specimens were determined using 0.1 mg accuracy digital weighing and digital caliper. The percent porosity was then converted directly from the density relative to the density of Si wafer (2.33 g cm^{-3}) according to the following equation:

$$\text{Porosity}(\%) = \left[1 - \frac{\left(\frac{\text{PS Weight}}{\text{PS Volume}}\right)}{\text{Density of Si wafer}}\right] \times 100 \quad (1)$$

3. Results and Discussion

3.1 Physical properties of coarsely crushed, fine, pressed and annealed PS

Figure 2 shows XRD spectra of (a) coarsely crushed Si powder, (b) mechanically ball-milled Si powder for 1 hour, (c) green compact PS pellet and (d) annealed PS pellets at 700 °C for one hour in H_2/Ar. From the XRD spectra, the sharp and strong peaks of (111), (220), (311), (400), and (331) planes were observed in the case of coarsely crushed silicon wafer, Figure 2(a). After ball milling for one hour, all peaks became boarder with the decrease of their intensities. After the pressing into a pellet at 4,000 psi, Figure 2(c), and then annealed at 700 °C for one hour in H_2/Ar, Figure 2(d), the XRD pattern became clearer. The crystalline size calculated from XRD spectra by the Scherer's equation were approximately 4, 6, and 10 nm for the mechanically ball-milled Si powder, green compacted Si pellet and annealed Si pellet at 700 °C for one hour, respectively. The improvement of crystalline size after the uniaxial pressing may not be significant because the energy from the pressing might not be enough to cause the grain growth. However, the annealing process after the pressing process might cause the grain growth and the increase of the crystalline sizes.

The SEM micrograph of an as-pressed PS pellet and an annealed PS pellet are shown in Figure 3(a) and (b), respectively. The SEM micrographs of as-pressed and annealed PS pellets at 700 °C for one hour were similar except the notice of slight charging effect in Figure 3(b). Micrographs show that the size of obtained particles varied from about 2-3 μm to less than 100 nm. Porosity was clearly observed from the samples.

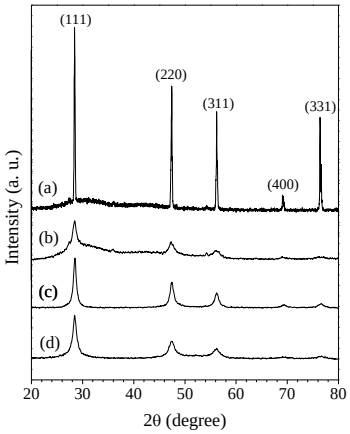

Figure 2. XRD spectra of (a) coarsely crushed Si powder, (b) mechanically ball-milled Si powder, (c) green-compacted PS pellet and (d) annealed PS pellet at 700 °C for 1 hour.

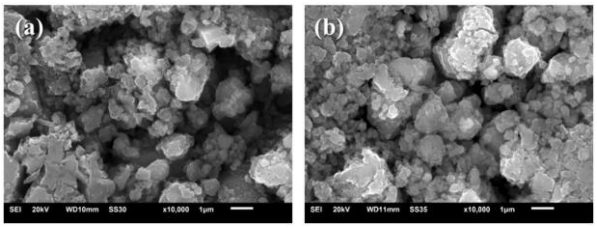

Figure 3. Surface morphology of (a) green-compacted PS pellet and (b) annealed PS pellet at 700 °C for 1 hour.

3.2 Effect of the milling time on the physical properties of PS pellets

The previous section showed that PS can be prepared using a simple powder method. Various grain sizes of silicon particles were observed in the samples after one hour milling. In this section, we investigated the effect of milling time on the physical properties of PS pellets. The attempt had been done in order to reduce the grain size and also improve the distribution of grain size at the same time. The silicon wafers were milled at various milling time from one to 21 hours.

The percent porosity of green compacted PS pellets varied from 39.2% to 43.5%. Also, it decreased about 1 to 2%, when the pellets were sintered. PS pellets became denser by the annealing process, possibly caused by the small grains annealed at the surface. Percent porosity of annealed PS samples decreased with the increase of the milling time as a result of grain size effect. For longer milling time, the time needed for sintering of particles decreased as a result of the decrease of grain size (Hosford, 2008). This was also the reason that when the milling time increased, the density of annealed PS pellets became higher than green compacted PS pellets.

Figure 4 shows that XRD patterns of the (a) as-pressed PS pellets at different milling time and (b) annealed Si pellet in H_2/Ar atmosphere at 700 °C for one hour. As ex pected, the intensity of the XRD spectra of the as-pressed pellets dropped with the boarder peak widths as the increase of the milling time. It indicated that the Si crystalline sizes

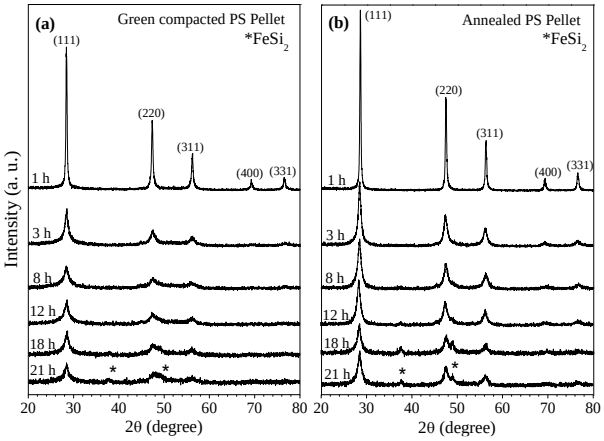

Figure 4. The XRD spectra of (a) green compacted PS pellet and (b) of annealed PS pellet in at 700 °C for 1 hour with various milling time.

became smaller. Note that the peak corresponding to (220) planes became broader than other peaks. The second phase of iron silicide ($FeSi_2$) was formed at the milling time starting from about 12 hours. That was the result from the mechanically alloying of silicon powder and part of iron ball. In Figure 4(b), after annealing in H_2/Ar atmosphere at 700 °C, the pellets showed stronger and sharper XRD spectra. Also, the second phase of tetragonal $FeSi_2$ was more pronounced. The (101) and (102) planes of $FeSi_2$ (JCPDS 35-0822) were clearly observed at 2θ of 37.6 and 48.9 degrees.

Figure 5 shows the relationship of the milling time and the crystalline size of green compacted and annealed Si pellets in H_2/Ar at 700 °C. From Figure 5, as the milling time increased from 1 to 21 hours, the crystalline sizes of green compacted PS calculated from Scherer's equation dropped from about 28 nm to about 5 nm. Note that the crystalline size dropped sharply during the first three hours of milling time. The crystalline size did not change significantly after 3-hour milling. In our case, the crystalline size was closely related to the grain size because the starting material of our mechanical ball milling process was single Si crystal wafer. Therefore, the crystalline size will decrease with the decrease of the Si powder size (grain size) with the increase of the milling time. The similar characteristics of the reduction of grain size with milling time were also shown in earlier work (Jakubowicz *et al.*, 2007). However, the crystalline sizes of all annealed specimens improved by 2 to 4 nm after the annealing at 700 °C for one hour. This confirmed that with a relative low

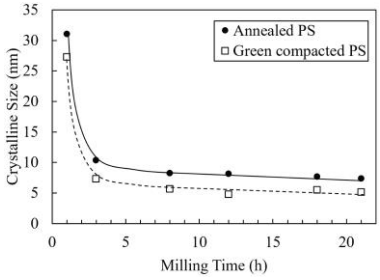

Figure 5. Relationship between crystalline size and milling time of green compacted PS pellet and annealed PS pellet at 700 °C for 1 hour.

temperature of 700 °C, the sintering process facilitated the joining of silicon nanoparticles. This could be indicated from the improvement of Si crystalline size. The calculated lattice parameter of Si varied between 0.539 and 0.545 nm corresponding to the reference lattice parameter of crystal Si of 0.543 nm. Only the slight decrease of the lattice parameter was observed as the milling time increased which reduced from 0.543 nm to 0.541 nm.

3.3 Effect of the annealing time and HF leaching on the physical properties of PS pellets

The annealing temperature was set at 900 °C for varying annealing time of 0.5, 1, 2, and 3 hours in order to induce the oxidation at the surface of the Si particles. The annealing temperature and time were estimated according to the graph from the oxide growth rate in dry oxygen (El-Kareh, 2002). The estimated oxide thickness were 60 nm and below at the temperature of 900 °C and with 3-hour oxidation time for <111> and <100> Si, respectively (El-Kareh, 2002). Figure 6 shows the XRD results of 1-hour ball-milled and annealed PS pellets for various times of 0.5, 1, 2, and 3 hours. The results indicated that, the increase of annealing time does not significantly change the XRD patterns. As shown in Figure 7, the crystalline size increased from 21 to 34 nm as the annealing time increased from 0.5 to 3 hours at 900 °C.

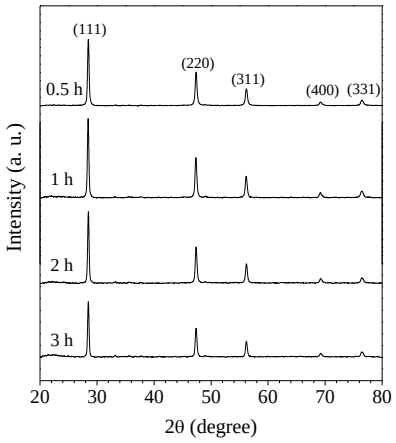

Figure 6. XRD spectra of annealed PS pellet at 900 °C with various annealing time.

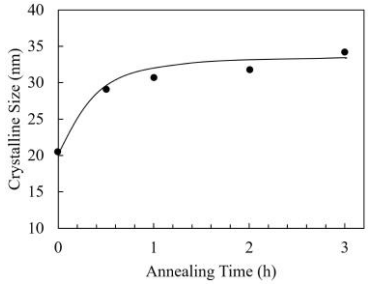

Figure 7. Relationship between crystalline size and annealing time of 1 hour ball-milled PS pellet temperature 900 °C.

The increase of crystalline size in Figure 7 was possibly caused by the bonds between contacting particles enlarged with the increase of sintering time (German, 1977). However, the Si crystalline size increased rapidly from 21 nm to 29 nm with the increase of annealing time from 0 to 1 hour. In contrast, after a 1-hour annealing time, the Si crystalline size increased slightly and became saturated. This might be because of the formation of oxide at the surface of the Si nanoparticles. Instead of binding nanoparticles together, the longer annealing time created thicker oxide layer which later confirmed by the presence of Si-O-Si bonding in FTIR (Figure 8).

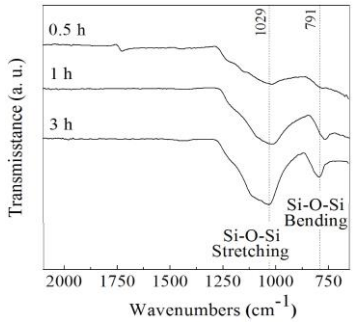

Figure 8. FTIR spectra of PS pellet before and after annealing with different annealing time at 900 °C.

The oxide film on the surface of the Si particles can be removed with the dilute HF solution to form a high surface area PS pellets. In this current study, the presence of oxidized silicon was observed using infrared absorption analysis. The bonding vibration of Si-O-Si stretching and Si-O-Si bending had been reported with position about 1,010–1,080 cm^{-1} and about 820 cm^{-1} (Jutarosaga *et al.*, 2005), respectively. In Figure 8, the transmission peaks corresponding to Si-O-Si stretching and Si-O-Si bending positioned at about 1,016–1,034 and 786–791 cm^{-1}, respectively. The FTIR spectra of annealed PS samples with the annealing time of 0.5, 1, and 3 hours at 900 °C in air were shown. The absorption of Si-O-Si bonding was more pronounced with the increase of the annealing time. Thus, the FTIR result was confirmed that silicon oxide was form during the annealing process.

Figure 9 shows the percent porosity of annealed PS pellet at 900 °C for one hour after HF leaching with various annealing time of about 0.5, 1, 2, and 3 hours. The results confirmed that, the percent porosity can be increased from 38.4 to 43.6% when soaking in 5% HF solution for 30 minutes for the sample annealed for two hours at 900 °C in air. However, there was no porosity data of the sample annealed for three hours at 900 °C in air after HF leaching. This was because the specimen cannot maintain the pellet shape after the leaching process. Numerous particles were instead observed after the etching process. It was suspected that the bonding between Si nanoparticles completely transformed to oxide layer and dissolved by HF solution during the etching process which caused the separations of Si particles.

Porosity could be mainly controlled by 1) the crystalline size, or particle size in this case, and 2) the oxidation of the surface of Si particles. As mentioned above that the crystalline size did not increase with the increase of annealing time at 900 °C in air due to the formation of oxide at the surface of Si powder, the small particle might become the oxide completely causing an unstable PS structure after leaching.

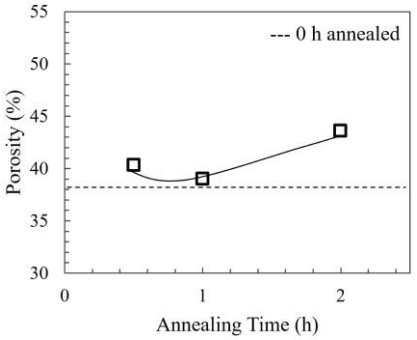

Figure 9. Relationship between porosity and annealing time of annealed PS pellet at 900 ºC after HF leaching.

Therefore, it is important to select the appropriate crystalline size of the powder samples and also the oxidation process to obtain the desired PS structure and porosity.

4. Conclusions

Bulk porous silicon (PS) was successfully fabricated using a simple ball-milling technique with the additional pressing, annealing in air to promote the oxidation and HF leaching technique to create larger pores by removing the oxide layer. Oxidizing the porous silicon can be indicated by the presence of Si-O-Si bonds in the specimens after annealing in air at 900 °C. This preliminary result shows the increase the porosity of PS from 38.4 to 43.6%. Further optimazation is needed in order to enhance the porosity of PS.

Acknowledgements

Authors would like to thanks P. Chanya for the supporting on the mechanical milling and the Office of the National Research Council of Thailand (NRCT) for providing funding for this research.

References

Ebrahimy, M. N., Orafaei, H. Andalib, A., & Alipuor-Banaei, H. (2015). Low power electro-optical filter: Constructed using silicon nanobeam resonator and PIN junction, *Physica E, 70*, 40–45.

El-Kareh, B. (2002). *Fundamentals of semiconductor processing technologies*. Massachusetts, MA: Kluwer Academic.

Epur, R., Minardi, L., Datta, M. K., Chung, S. J, & Kumta, P. N. (2013). A simple facile approach to large scale synthesis of high specific surface area silicon nanoparticles. *Journal of Solid State Chemistry, 208*, 93–98.

Hosford, W. F. (2008). *Materials for engineers*. New York, NY: Cambridge University Press.

German, R. M. (1977). *Powder metallurgy science*. Princeton, NJ: Metal Powder Industries Federation.

Jakubowicz, J., Smardz, K., & Smardz, L. (2007). Characterization of porous silicon prepared by powder technology. *Physica E, 38*, 139–143.

Ji, K. S., Choi, J., Yang, H., Lee, H. M., & Kim, D. (2011). A study of crystallinity in amorphous Si thin films for silicon heterojunction solar cells. *Solar Energy Materials and Solar Cells, 95*, 203–206.

Jutarosaga, T., Jeoung, J. S., & Seraphin, S. (2005). Infrared spectroscopy of Si-O bonding in low-dose low-energy separation by implanted oxygen materials. *Thin Solid Films, 476*, 303–311.

Kim, H., & Cho, N. (2012). Morphological and nanostructural features of porous silicon prepared by electrochemical etching. *Nanoscale Research Letters, 7*(1), 1-8.

Kurdi M. E., Boucaud, P., Sauvage, S. Fishman, G., Kermar rec, O., Campidelli, Y., . . . Sagnes, I. (2003). Silicon-on-insulator and SiGe waveguide photodetectors with Ge/Si self-assembled islands. *Physica E, 16*, 523-527.

Moiz, S. A., Nahhas, A. M., Um, H. D., Jee, S. S., Cho, H. K., Kim, S.W., . . . Lee, J.H. (2012). A stamped PEDOT: PSS–silicon nanowire hybrid solar cell. *Nanotechnology, 23*, 145401.

Naddaf, M., & Hamadeh, H. (2009). Visible luminescence in photo-electrochemically etched p-type porous silicon: Effect of illumination wavelength. *Materials Science and Engineering: C, 29*, 2092–2098.

Russo, L., Colangelo, F., Cioffi, R., Rea, I., & Stefano, L. D., (2011). A mechanochemical approach to porous silicon nanoparticles fabrication. *Materials, 4*(6), 1023-1033.

Salman, K. A., Omar, K., & Hassan, Z. (2011). The effect of etching time of porous silicon on solar cell performance. *Superlattices and Microstructures, 50*, 647–658.

Salman, K. A., Omar, K., & Hassan, Z. (2012). Effective conversion efficiency enhancement of solar cell using ZnO/PS antireflection coating layers. *Solar Energy, 86*, 541–547.

Serov, M. M. (2014). *Structural properties of porous materials and powders used in different fields of science and technology*, London, England: Springer.

Smestad, G., Kunst, M., & Vial, C. (1992). Photovoltaic response in electrochemically prepared photoluminescent porous silicon. *Solar Energy Materials and Solar Cells, 26*, 277–283.

Stelzner, T., Pietsch, M., Andra, G., Falk, F., Ose, E., & Christiansen, S. (2008). Silicon nanowire-based solar cells. *Nanotechnology, 19*, 295203.